

A New Circular Polarization Metamaterial Ferrite Phase Shifter

Meisam Shafaei, Seyed Mohammad Javad Razavi, Emad Hamidi

Engineering University Complex (EEEUC), Malek-e-Ashtar University of Technology (MUT), Tehran, Iran,
Emails: meisam.shafaei@gmail.com, razavismj@mut.ac.ir, emadhamidi@iran.ir

Corresponding author: razavismj@mut.ac.ir

Abstract- In this paper, a new X band Metamaterial (MTM) based ferrite phase shifter is presented. The phase shifter is excited by circular polarized wave base on combination of TE_{10} and TE_{01} modes in a square waveguide. In order to synthesize negative index material (NIM), negative permeability of ferrite slabs in extraordinary mode is mixed with the negative permittivity of printed periodic metallic wires on substrate, in the same frequency band. By using the introduced new circular polarized MTM based layout, the proposed phase shifter loss is less than 3 dB, while the loss of MTM waveguide phase shifters is about 10 dB. Also, the proposed phase shifter profits the miniaturization property of MTM design usage. The total length of the phase shifter is 2 cm with 360° differential phase shift, compared to common dual mode phase shifter with 6 cm length in X band.

Index Terms- phase shifter, metamaterial, circular polarization, insertion loss, and miniaturization.

I. INTRODUCTION

Metamaterial phase shifters are recently presented and studied after the huge electromagnetic mutation of “Metamaterials” which introduced by pendry and implemented by Smith et.al for the first time. Not only the extraordinary features of left handed material interested the physicists and scientists to explore their properties, but the engineers were excited to use such a unique specification of them in practical projects and devices. Miniaturizing that is a left handed property, could be used in phase shifters size compression. Bandwidth enhancement is one of the other metamaterial profits, also. The Zero-degree phase shift achievement is another property of the reported MTM phase shifters.

The last property is dedicated for broadside antenna array excitation applications, where feeding phase of each element is assumed the same (for example zero degree). But passing the wave through the ordinary microwave components, enforces the phase shift more than zero degree ($\Delta\phi_{RHM}$), therefore the next acceptable value is -360 degrees, which makes the phase shifter very long and bulky; while using left handed materials with negative propagation constant in contrast with right

handed materials, enables the designer to compensate the $\Delta\varphi_{RHM}$, with $\Delta\varphi_{LHM}$ with opposite sign in much shorter length, that leads to zero degree phase in a very compact phase shifter, for example 12 times shorter for X band phase shifter [11,12].

For expressing a brief overview on MTM phase shifters, the transmission line (TL) phase shifter implementation should be mentioned because of its straightforward design and simple realization method, which considered by many MTM phase shifter designers [5-10]. The unit-cell of MTM phase shifter could be implemented via either lumped circuit element, or using microwave substrate distributed circuit. The unit-cell dimensions should be short enough that the medium could be seen with an effective permittivity and permeability from electromagnetic point of view. So, usually the unit-cell length is assumed one tenth of the wave length or shorter. The other alternative for TL implementation consists spatial unit-cell positioning inside the waveguide framework.

The lumped element realization can be used for fixed [10] or variable [8] differential phase shifts. In MTM variable phase shifters, the phase shift can be tuned by a controllable component, such as tuning the phase shift by impedance varying of semiconductor devices continuously [8] or the discrete levels as on and off states [9].

By exceeding the frequency, according to the explained unit-cell length limit, the substrate MTM phase shifter layout could be used [10, 12]. But the substrate thickness is an important power handling constrainer parameter. Therefore, the waveguide MTM phase shifter frameworks with spatial unit-cell design method could be used for high power applications [5-7].

In linear polarization (LP) radars, the changes in polarization of scattered wave from the target cause changes in the received signal level due to the inability of the linear polarized antennas to receive polarization changes. Based on Touzi's findings, Circular Polarization (CP) radars are more powerful for ships detection in compared with LP radars [18]. Furthermore, CP waves can survive Faraday rotation effect in ionosphere communications such as low frequency L-band LP-SAR satellites or in over the horizon (OTH) radars. Because of the useful features of CP waves and microwave systems, there is a growing trend in current Laboratory researches or modern technologies such as S300, unmanned aerial vehicle (UAV), aircraft, and microsatellite platforms [17]. Therefore, using circular polarization phase shifters in those microwave systems without adding any lossy polarization converter devices, would be a good plan.

In the next section the metamaterial mechanism of the proposed phase shifter will be investigated and approximate 1D design will be addressed analytically in linear polarization excitation state. Then, by applying some mathematical equation derived from physical orthogonality symmetry, the analytic CP results obtained. After that, the full wave software simulation results will be presented in section 3; and at the last, in the conclusions section the microwave achievements of the new proposed phase shifter will be discussed and compared to the other left/right handed material phase shifters.

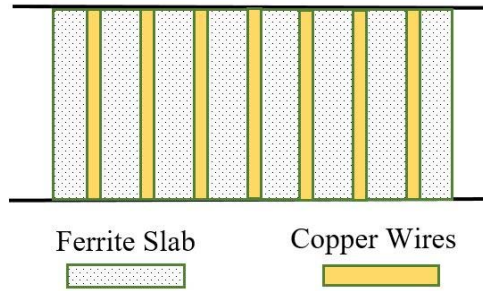


Fig. 1. Metamaterial configuration scheme (longitude section of the waveguide).

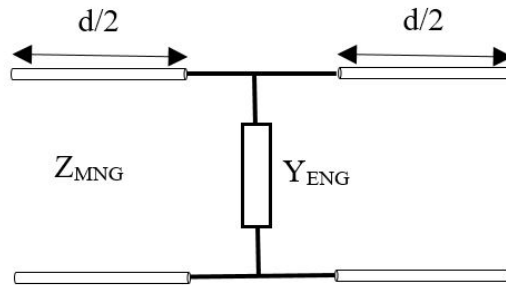


Fig. 2. Equivalent circuit of the metamaterial structure unit-cell.

II. METAMATERIAL CORE DESIGN

For composing the synthetic negative refraction index medium, two epsilon-negative (ENG) and mu-negative (MNG) substructures are designed and assembled, which illustrated in Figure 1. In the design procedure, an electromagnetic solver should be used. Several options such as analytic solution based on numeric electromagnetic code development or full wave software simulations exists. The analytic solver uses one dimensional TEM approximation and transfer function matrix (TFM) method [15] that would be explained in this section. A designer could benefit both analytic and software simulation method so that for the initial parameters tuning, the analytic method with less time consuming could be applied. In this level the effect of each parameter variation gives the researcher a good design insight. Finalizing the optimized parameters could be done by more accurate full wave method via commercial software. The metamaterial configuration and analytic solution will be explained here.

In order to build ENG structure, the periodic metallic wires are aligned in parallel positions. The dimensions of each wire regarded to the wavelength is small enough that it is considered as a lumped unit-cell element. The Equivalent circuit of the above structure's unit-cell is shown in Figure 2.

Where Y_{ENG} denotes for copper wires admittance, and Z_{MNG} is intrinsic impedance of equivalent transmission line corresponding to the ferrite slab. The parameter d is the distance between the periodic wires, or in the other words, it is unit-cell length.

The conductive wire admittance could be obtained by equation below:

$$Y_{ENG} = \left(\frac{1}{2\pi r \left(\sqrt{\frac{\omega\mu_0}{2\sigma}} \right)^{(1-i)} - i\omega\mu_0 l \left(\frac{\ln\left(\frac{d}{r}\right)}{2\pi} \right)} \right)^{-1} \quad (1)$$

Where, l indicates for wire length, r is wire radius, σ is wire conductance. In a similar way, the impedance of MNG structure is:

$$Z_{MNG} = \sqrt{\mu_e/\epsilon} \quad (2)$$

When, according to the μ and κ of ferrite tensor definition the effective permeability of ferrite slabs in extraordinary bias $\mu_e = \frac{\mu^2 - \kappa^2}{\mu}$, and ϵ is the ferrite dielectric constant [2,3].

The transfer function of the equivalent TL with the impedance Z_{MNG} , wave number $k = \omega\sqrt{\mu_e\epsilon}$ with the length $d/2$ in either side of the lumped shunt admittance Y_{ENG} , can be obtained by equation (3).

$$A_{MNG} = \begin{bmatrix} \cos\left(\frac{kd}{2}\right) & -iZ_{MNG} \sin\left(\frac{kd}{2}\right) \\ -\frac{i \sin\left(\frac{kd}{2}\right)}{Z_{MNG}} & \cos\left(\frac{kd}{2}\right) \end{bmatrix} \quad (3)$$

Where, the Transfer function of the shunt lumped ENG element is:

$$A_{ENG} = \begin{bmatrix} 1 & 0 \\ Y_{ENG} & 1 \end{bmatrix} \quad (4)$$

After determining two ENG and MNG substructures, now the total transfer function of the DNG ($\epsilon < 0$, $\mu < 0$) structure containing N unit-cells can be represented.

$$A = (A_{MNG}A_{ENG}A_{MNG})^N \quad (5)$$

By using simple mathematical works the scattering matrix of the structure can be extracted from the matrix A [9, 13]. Then, by applying reversion algorithms on scattering parameters the equivalent refractive index n , and equivalent permittivity ϵ , and permeability μ of the mentioned two port network could be obtained [5,11].

The mentioned algorithm application on a candidate unit-cell with the properties of: $l=2$ mm, $r=0.15$ mm, $d=2$ mm, $N=10$, $4\pi M_s=2100$ Gauss, $\epsilon_r=15.5$, $\Delta H=250$ Oe and $H_0=1000$ Oe. is carried out and the effective permittivity, permeability and refractive index is illustrated in the next figures.

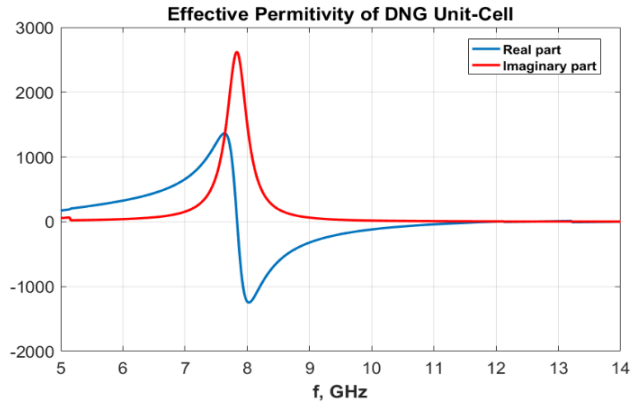


Fig. 3. Real and imaginary part of effective permittivity of the MTM unit-cell.

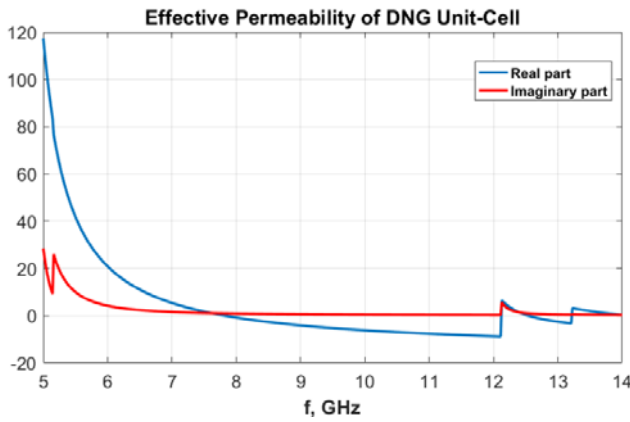


Fig. 4. Real and imaginary part of effective permeability of the MTM unit-cell.

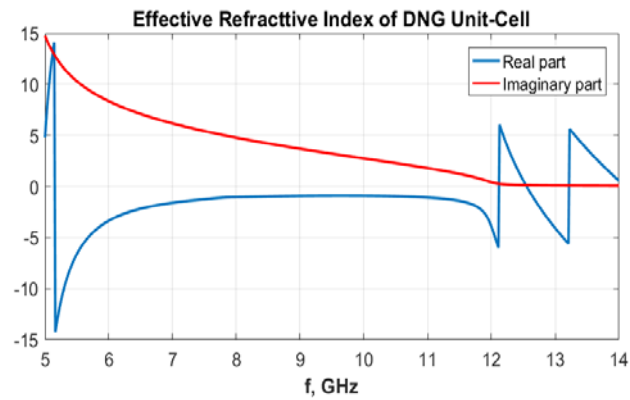


Fig. 5. Real and imaginary part of effective refractive index of the MTM unit-cell.

An important phenomena that is studied in many references, is the adjustable MTM unit-cell matter [19] that could be composed of ferrite substrate whose left handed properties easily could be controlled and shifted by external DC magnetic field (H_0). Since this topic is not directly related to the author’s main contribution, it has been left to the future works.

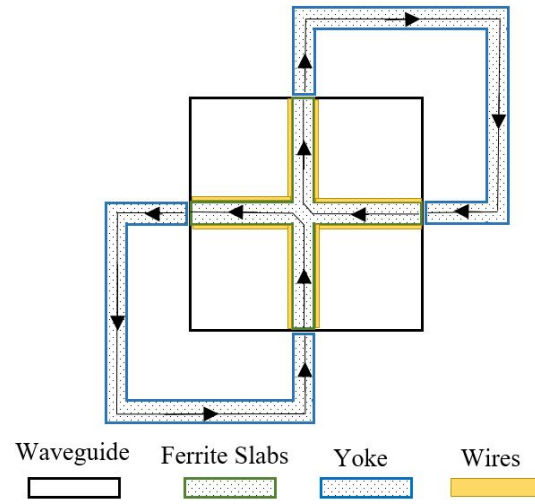


Fig. 6. Cross section view of magnetic bias field directions.

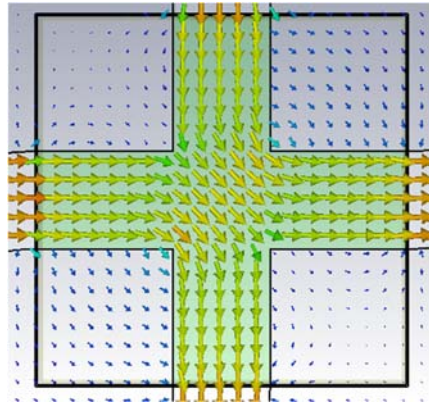


Fig. 7. DC Magnetic Field direction inside the phase shifter

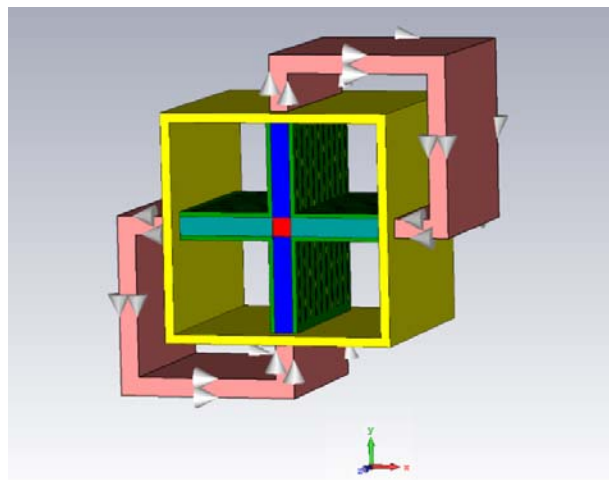


Fig. 8. The plus, "+", Phase Shifter configuration.

III. PROPOSED PHASE SHIFTER

The Proposed phase shifter housing includes square waveguide which excited by two orthogonal TE₁₀ and TE₀₁ modes with 90 degrees time shift that causes a circular polarized wave. Since the circular polarization wave is combination of two linear waves with 90 degrees of physical angle, a symmetric plan for each linear polarization wave vectors would be an initial guess for phase shifter design choice. After examining several orthogonal structures, the structure plus, “+” that is composed of two ferrite slabs with the early satisfactory results have been chosen according to Figure 6.

As shown in Figure 6, the magnetic flux enforced by wire winding around the ferrite yokes, yields two closed loop flux paths. The orthogonal magnetic bias field inside the ferrite slabs is almost constant and in one direction in each slab, as desired.

The Magnetostatic analysis of the phase shifter is accomplished by using nonlinear B-H hysteresis curves in Microwave CST Magnetic Solver environment whose visual results is demonstrated in Figure 7.

After Magnetostatic (DC) simulation and obtaining permeability tensor of the anisotropic ferrite material, the electromagnetic full wave (RF) analysis could be applied. Based on magnetic field bias amplitude regarded to the saturation magnetization value of the ferrite material, the Polder [15] or Green and Sandy model [16] is used for full magnetized or partial magnetized states, respectively.

In order to compose the synthetic NRI medium, the ferrite slabs are biased transversely (regarded to the wave passing direction) which is called extraordinary excitation mode with negative permeability (MNG). On the other side for composing negative permittivity medium, printed periodic copper wires on the substrate is used in the way that the wires are parallel to the electric field polarization and periodicity vector is aligned in the wave propagation direction as shown in Figure 8.

The circular polarization results could be extracted from combining the results of two orthogonal linear polarization modes with the same amplitude and 90 degrees phase shift. The amplitude and the phase of circular polarization wave could be derived according to the below equations.

$$|S_{21}^{CP}| = \sqrt{\frac{|S_{21}^{(1)(1)} \pm jS_{21}^{(1)(2)}|^2 + |S_{21}^{(2)(1)} \pm jS_{21}^{(2)(2)}|^2}{2}} \quad (6)$$

$$\angle S_{21}^{CP} = \angle \left(\frac{S_{21}^{(1)(1)} \pm jS_{21}^{(1)(2)}}{\sqrt{2}} \right) \quad (7)$$

$$S_{ij}^{(m)(n)} \triangleq \frac{V_i^{-(m)}}{V_j^{+(n)}} \quad (8)$$

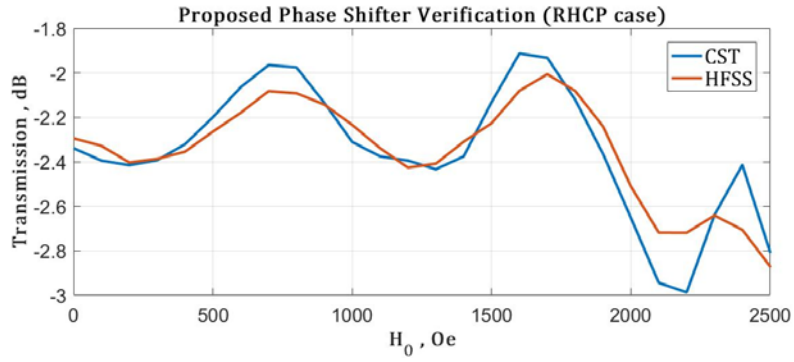


Fig. 9. CST and HFSS results comparison for amplitude of transmission wave versus bias magnetic field.

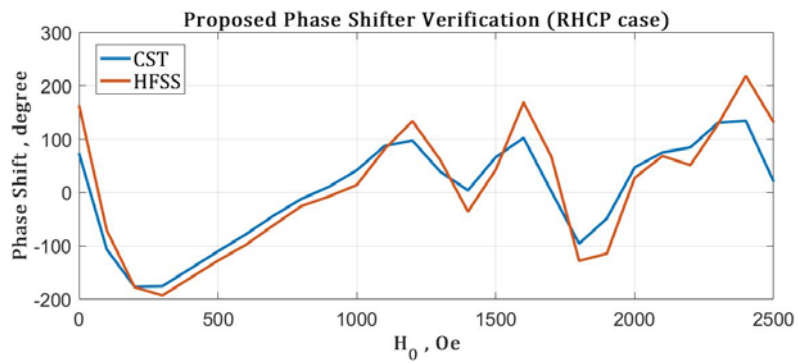


Fig. 10. CST and HFSS results comparison for phase shift of transmission wave versus bias magnetic field.

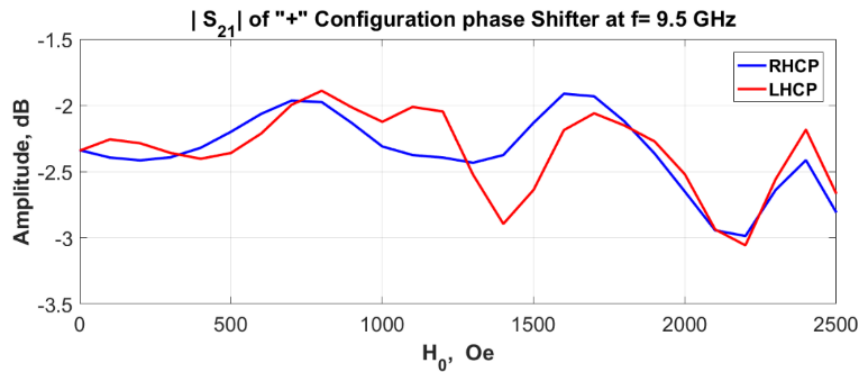


Fig. 11. Amplitude of transmission wave versus bias magnetic field

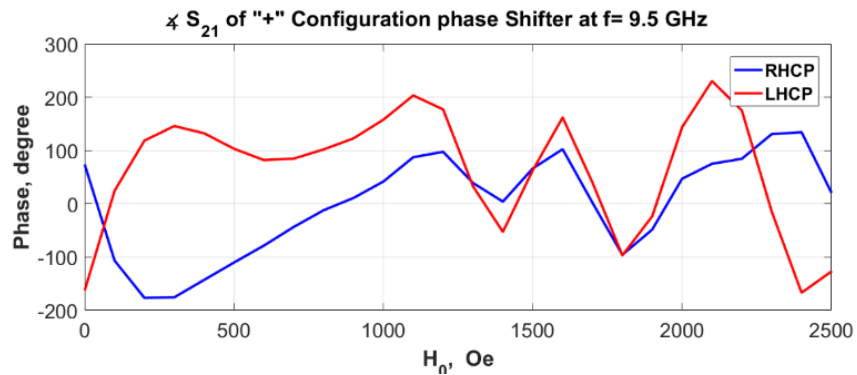


Fig. 12. Phase shift of transmission wave versus bias magnetic

Where $V_i^{-(m)}$ denotes for the outward wave leaving port #i in mode #m and $V_j^{+(n)}$ denotes for the inward wave flows through port #j in mode #n. The sign \pm in equations (6) and (7) is assigned for the right hand circular polarization and the left hand circular polarization waves, respectively. The combined extracted results, could be obtained by using simultaneous excitations of two orthogonal modes in CST, which leads to the exactly same results as calculated by equations (6) and (7).

One of the most important ferrite characteristic parameters is $4\pi M_s$ value that is determined by frequency band so that $\frac{\gamma 4\pi M_s}{\omega}$ should be around 0.4 to 0.6 [16]. The length of ferrite core is strongly related to $4\pi M_s$ value. By using the ferrite with higher $4\pi M_s$, one can decrease the ferrite core length, but on the other side the magnetic loss increases [16], then the $4\pi M_s$ could be increased as long as insertion loss dose not rise noticeably.

Based on required power handling capability and DC bias parameters that directly depends on B_r and H_c of hysteresis loop, the ferrite type could be determined. So the ferrite material XL21A based on the global source company catalogue standard is used, whose $4\pi M_s$ is 2100 Gauss, ϵ_r is 15.5 and its ΔH is equal to 250 Oe.

After some local electromagnetic and physical parameters optimizations as discussed in section 2, the optimized parameters is archived in order to decrease the insertion loss and increase the differential phase shift. The thickness of ferrite slabs and the longitudinal length of the slabs are 1 mm and 20 mm, respectively. The width and height of square waveguide is assumed 10.16 mm. In the first step, for verifying the Microwave CST software results, the amplitude and phase of RHCP case has been simulated by HFSS finite element base also. The corresponding results are demonstrated in figures 9 and 10.

As one may see, the results of two different strong full wave Electromagnetic simulators, are quite close and acceptable. So, the insertion loss and differential phase shift results of right and left circular polarizations are presented in Figure 11 and Figure 12.

As shown in the figures 11 and 12 for bias magnetic field range 0-2.5 kOe the maximum insertion loss is about 3 dB, when in the same range the differential phase shift of 360° is available for both RHCP and LHCP. The 3 dB loss for a MTM phase shifter would be an excellent result since one of the most disadvantages that suffers waveguide MTM phase shifter is high insertion loss factor so that the loss of X band MTM phase shifter is about 6 to 10 dB [7]. For addressing the results of proposed phase shifter, it has been compared with two MTM and one conventional right handed industrial phase shifter in table 1.

Table 1. Comparison of the proposed Phase Shifter properties with other MTM and Conventional Phase Shifters

Phase Shifter Type	Frequency (GHz)	Ferrite length	Polarization, Mode	Insertion Loss (dB)	Phase Shift (Degrees)	Magnetic Bias Field (kOe)
Dual Mode [21]	X band	~ 60 mm rod	LCP	< 1.5	360	< 0.1
MTM [7]	8.7	12 mm 3 pieces	Linear (TE ₁₀)	11-27	160	3-4
MTM [20]	9	8.5 mm 2 pieces	Linear (TE ₁₀)	6-10	45	3-5
Proposed Phase Shifter	9.5	20 mm 2 pieces	CP (TE ₁₀ + TE ₀₁)	< 3	360	< 2.5

Another important problem of the waveguide MTM phase shifter is high magnetic bias field amplitude requirement. A practical dual mode X band phase shifter could simply drive by maximum 150 mA current and appropriate wire winding turn (about 50 turns). But in previous MTM phase shifters [5-7], the bias magnetic field of order 7 kOe should be provided. By considering the size of mentioned phase shifters, the bias current winding of 300000 ampere turns is required, that only could be provided in experimental environments. As one can see, the required bias magnetic field of proposed phase shifter is reduced half of the similar phase shifters. The bias magnetic field may be applied by the wire winding around ferrite yokes shown in Figure 4, such that magnetic flux of slabs see much less reluctance, because the magnetic flux flows through the ferrite medium instead of air with much higher reluctance. The critical point of DC bias involves reducing the gaps placed between the ferrite core slabs and the yokes as short as possible in order to decrease the DC power supply current or reducing the wire winding turns.

IV. CONCLUSIONS

Since the proposed phase shifter works for circular polarization wave, the need of using polarizer in the either end of the phase shifter for converting the linear polarization wave to the circular polarization and vice versa has been removed.

The proposed phase shifter with 20 mm length in comparison with the standard X band dual mode phase shifter with about 70 mm length and single toroid phase shifter with about 100 mm, it is very short. The benefits of miniaturization factor will be more important in ground based radars with more than 10k elements, whose weight and size would be a great electromechanical challenge.

As mentioned in previous section, the waveguide MTM phase shifters, suffer from two important points. First, high insertion loss and second, much bias magnetic field requirements. The proposed phase shifter reduces the insertions loss to 3 dB in comparison with similar MTM phase shifters with 6 to 10 dB loss. And the providing bias field is reduced to one third of this kind phase shifters. By somewhat healing these two practical problems of MTM phase shifters and also new open fields that introduced in this paper such as circular polarization use of MTM phase shifters, there is more hopes

for practical use of waveguide MTM phase shifters rather than pure academic research and development works in experimental environments.

ACKNOWLEDGMENT

The authors would like to thank Prof. Shibani K. Koul for his guidance and responding to the author's questions by patience, regarded to his tight schedules.

REFERENCES

- [1] D. Parker and D. C. Zimmermann, "Phased arrays-part II: implementations, applications, and future trends," in *IEEE Transactions on Microwave Theory and Techniques*, vol. 50, no. 3, pp. 688-698, March 2002.
- [2] Collin RE. "Foundation for Microwave Engineering". 2nd ed. Cleveland, OH: IEEE Press, Wiley; 2001.
- [3] Pozar DM, "Microwave Engineering", 4th ed. Hoboken, NJ: Wiley; 2012.
- [4] M. A. Abdalla and Z. Hu, "Ferrite tunable metamaterial phase shifter," 2010 IEEE Antennas and Propagation Society International Symposium, Toronto, ON, 2010, pp. 1-4.
- [5] He P, Parimi PV, He Y, Harris VG, Vittoria C, "Tunable negative refractive index metamaterial phase shifter", *Electron Lett.* 2007;43 (25):1440-1441.
- [6] Peng He PV, Parimi H, Mosallaei VGH, Vittoria C, "Tunable negative refractive index metamaterial phase shifter", *IEEE Antennas and Propagation Society International Symposium*; 1725-1728;2007.
- [7] Peng He, Jinsheng Gao, P. V. Parimi, C. Vittoria, and V. G. Harris, "Tunable Negative Refractive Index Metamaterials and Applications at X and Q-bands", DARPA-APO funded project at U.S. Army Research Office, 4300 S. Miami Blvd, Durham NC 27703, MARCH 2008.
- [8] Tork HS. "Tunable Ferroelectric Meta-Material Phase Shifter Embedded Inside Low Temperature Co-Fired Ceramics (LTCC)" [Ph.D. dissertation]. Dept. ECE, University of Idaho; 2012.
- [9] Michael Maassel, "A metamaterial-based multiband phase shifter", [Ph.D. Dissertation], Dept. ECE, North Dakota State University of Agriculture and Applied Science, Fargo, October 2013.
- [10] M. A. Antoniadis and G. V. Eleftheriades, "Compact linear lead/lag metamaterial phase shifters for broadband applications," in *IEEE Antennas and Wireless Propagation Letters*, vol. 2, pp. 103-106, 2003.
- [11] Engheta N, Ziolkowski RW, "Metamaterials, Physics and Engineering Explorations", Piscataway, NJ: IEEE Press, Wiley Interscience; 2006.
- [12] M. A. B. Abbasi, M. A. Antoniadis and S. Nikolaou, "A Compact Reconfigurable NRI-TL Metamaterial Phase Shifter for Antenna Applications," in *IEEE Transactions on Antennas and Propagation*, vol. 66, no. 2, pp. 1025-1030, Feb. 2018.
- [13] Xudong Chen, Tomasz M. Grzegorzczak, Bae-Ian Wu, Joe Pacheco, Jr., and Jin Au Kong", Robust method to retrieve the constitutive effective parameters of metamaterials", *Phys. Rev. E*, vol. 70, no. 1, pp. 016608-016614, July 2004.
- [14] Magnus W. Haakestad and Johannes Skaar, "Causality and Kramers-Kronig relations for waveguides", *Optical Society of America*, Vol. 13, No. 24. 28 November 2005.
- [15] C. Vittoria, "Elements of Microwave Networks, Basics of Microwave Engineering", World Scientific publishing, Farrer Road Singapore, 1998.
- [16] Shibani K. Koul, Bharathi, "Microwave and Millimeter Wave Phase Shifters: Dielectric and Ferrite Phase Shifters", Volume I. Boston, MA: Artech House; 1991.
- [17] Yuta Izumi, Sevket Demirci, Mohd Z. Baharuddin, Josaphat T. S. Sumantyo, and Heein Yang, "Analysis of Circular Polarization Backscattering and Target Decomposition Using GB-SAR", *Progress In Electromagnetics Research B*, Vol. 73, 17-29, 2017.

- [18] R. Touzi and F. Charbonneau, "Requirements on the calibration of Hybrid-Compact SAR," 2014 IEEE Geoscience and Remote Sensing Symposium, Quebec City, QC, 2014, pp. 1109-1112.
- [19] Yang Yong-Jun, Huang Yong-Jun, Wen Guang-Jun, Zhong Jing-Ping, Sun Hai-Bin and Oghenemuro Gordon, "Tunable broadband metamaterial absorber consisting of ferrite slabs and a copper wire", Chin. Phys. B Vol. 21, No. 3 (2012).
- [20] Peng He, "Tunable Ferrite-Based Negative Index Metamaterials for Microwave Device Applications", [Ph.D. Dissertation], Electrical Engineering, Northeastern University Boston, Massachusetts December 2009.
- [21] Microwave applications group, "Dual-Mode Phase Shifters Data Sheet", www.magsmx.com, 3030 Industrial Parkway, Santa Maria, California 93455 • (805) 928-5711.